Solid State Communications 250 (2017) 70–74

Contents lists available at ScienceDirect

Solid State Communications

journal homepage: www.elsevier.com/locate/ssc

Communication

Stacking-dependent transport properties in few-layers graphene

Matheus Paes Lima[a], José Eduardo Padilha[b,*], Renato Borges Pontes[c], Adalberto Fazzio[d,e], Antônio José Roque da Silva[f,g]

[a] Departamento de Física, Universidade Federal de São Carlos, CP 676, 13565-905, São Carlos, SP, Brazil
[b] Universidade Federal do Paraná, Campus Avançado de Jandaia do Sul, Jandaia do Sul, PR, Brazil
[c] Instituto de Física, Universidade Federal de Goiás, Campus Samambaia, 74690-900, Goiânia, GO, Brazil
[d] Instituto de Física, Universidade de São Paulo, CP 66318, 05315-970, São Paulo, SP, Brazil
[e] Centro de Ciências Naturais e Humanas, Universidade Federal do ABC, Santo André, São Paulo, Brazil 09210-170
[f] Instituto de Física, Universidade de São Paulo, CP 66318, 05315-970, São Paulo, SP, Brazil
[g] Laboratório Nacional de Luz Síncrotron, CP 6192, 13083-970, Campinas, SP, Brazil

ARTICLE INFO

Keywords:
A. Few layers graphene
D. Stacking sequence
D. Electronic Transport Properties
E. First-Principles Calculations

ABSTRACT

By performing *ab initio* electronic structure and transport calculations, we investigated the effects of the stacking order (Bernal (AB) and rhombohedral (ABC)) as well as the number of layers, in the electronic structure and charge transport of few-layers graphene (FLG). We observed that for the ABC stack the transport properties are derived from surface states close to the Fermi level connected to dispersive states with an exponential penetration towards the inner layers, whereas for the AB stacking the transport is distributed over all layers. We present a simple model for the resistances as a function of the number of layers which contemplates the different contribution of the surface and inner layers for the transport. However, even if the stackings AB and ABC present completely different electronic and transport properties, both present the same cohesive energies, showing the absence of a thermodynamical preference for a given kind of stacking.

1. Introduction

The potential to produce new systems with improved performance via stacking of weakly interacting two-dimensional (2D) materials is attracting increasing attention [1–7]. These so-called van der Waals crystals may open up new vistas towards nano devices with better properties. Graphene was the first 2D material to be synthesised, about 10 years ago [8], which spurred a wealth of research with both basic as well as applied objectives. Since then, many other 2D materials were also obtained, and many combinations between them have been proposed and fabricated. Besides the kinds of 2D sheets to be stacked, it is to be expected that the properties of these systems will depend both on the number as well as on the orientation of these layers. In this sense, the stacking of few layers of graphene (FLG) can be viewed as a limiting case of such combinations where there is only one single kind of 2D material. This simplifies the analysis and highlights the importance of number of layers and stacking order.

FLGs have by themselves also attracted attention in recent years [9–13]. There are two natural stacking orders that are mostly observed: the AB (or Bernal), and the ABC (or rhombohedral). As discussed, it is possible to tune the electronic structure in these materials by changing both the number of layers and/or the stacking order [14–18]. One of the outstanding differences between the AB and the ABC stacking is the presence of highly localised surface states only in the latter case [19]. Even though stacking dependent transport properties of FLGs have been experimentally investigated [20–22], these studies have focused only in a very few specific number of layers. Thus, a clear connection between the electronic structure and the transport properties, and how they evolve with number of layers and stacking order is still lacking.

In this article we bridge this knowledge gap by presenting a clear understanding of the source of the differences in the electronic and transport properties of FLGs. We show that a strong dependence of the electronic and transport properties on the kind of stacking occurs because for the ABC stacking pattern there is a strong contribution from flat surface states around the Fermi level (E_F) connected to dispersive states with an exponential penetration to the inner layers, whereas for the AB stacking only dispersive bulk states delocalised over all layers are involved. As a consequence, the behaviour of the current with the number of layers (N) can be well described in terms of a simple model of sum of resistances in parallel. For the AB stacking

* Corresponding author.
E-mail addresses: mplima@df.ufscar.br (M.P. Lima), jose.padilha@ufpr.br (J.E. Padilha), pontes@ufg.br (R.B. Pontes), fazzio@if.usp.br (A. Fazzio), jose.roque@lnls.br (A.J.R.d. Silva).

http://dx.doi.org/10.1016/j.ssc.2016.11.012
Received 21 October 2016; Accepted 13 November 2016
Available online 20 November 2016
0038-1098/

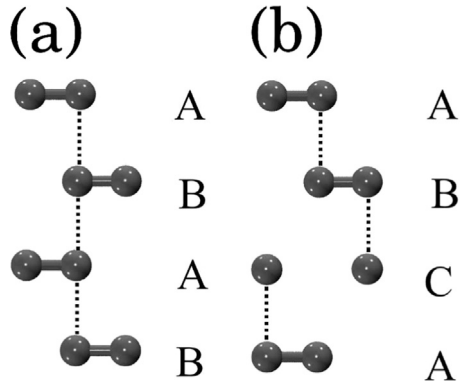

Fig. 1. Schematic representation of the FLG in the (a) AB and (b) ABC stacking patterns, exemplified for N=4.

there are N equally contributing resistances, whereas for the ABC the inner layer resistances have exponentially decreasing contributions. Furthermore, despite all these very different qualitative and quantitative electronic structure and transport properties, both stacking configurations present the same interlayer cohesive energy, indicating the absence of a thermodynamical preference for a given kind of stacking.

2. Computational details

In Figs. 1 (a) and (b) we show a schematic representation of the AB and ABC stacking order. The relative atomic positions between any two nearest neighbour layers are the same for the two stackings. However, for greater distances the relative positions are different. In order to obtain the structures to be used in the electronic structure and transport calculations, we performed total energy *ab initio* simulations based on the Density Functional Theory (DFT). We fully relaxed the geometries considering the Local Density Approximation [23] (LDA), as implemented in the SIESTA code [24]. The simulation parameters were optimized for a precision in the total energy of $\pm 0.2 \times 10^{-4}$ meV. We used 400 Ry for the mesh cutoff, 0.005 eV/Å for the force relaxation criterion, a *DZP* basis set and a set of 50×50 k-points in the unit cell to represent the Brillouin zone of the system. Our simulations, in accordance to other works [16,25,26], show that the LDA functional lead to an interlayer distance of 3.22 Å, which is close to the experimental value for bulk graphite (3.33 Å [27]), as well as to an accurately description of the energy bands around E_F.

In the ballistic regime, the transport properties of pristine systems in general can be obtained by a simple counting of bands, and this is the case of the geometries here investigated. However, to get the numerical values for the electrical currents, we performed ballistic transport calculations for FLG up to 12 layers, in the both Bernal and ABC stacking patterns. We choose this procedure to be sure to take in account thin details of the energy bands in the transport window that can be important for the evolution of the electrical current with the number of layers.

The electronic transport properties were calculated within the Landauer–Büttiker formalism [28–30]. The Hamiltonian for the system was obtained combining non-equilibrium Green's functions with *ab initio* density functional theory (NEGF-DFT), as implemented in the TRANSAMPA code [31–33]. We used a source drain voltage of 50 mV, comparable to the bias voltages used in the experiments [34] and the calculations were done at room temperature. To calculate the current we performed a fully self-consistent NEGF-DFT calculation with zero-bias, and then used the linear response approximation, which is accurate enough to describe the flowing current at low bias. The system used in our transport calculations is depicted in Fig. 2 (a). To account for the 2D-structure of the FLG, we considered 10,000 k-points transversal to the transport direction ($k_\perp$).

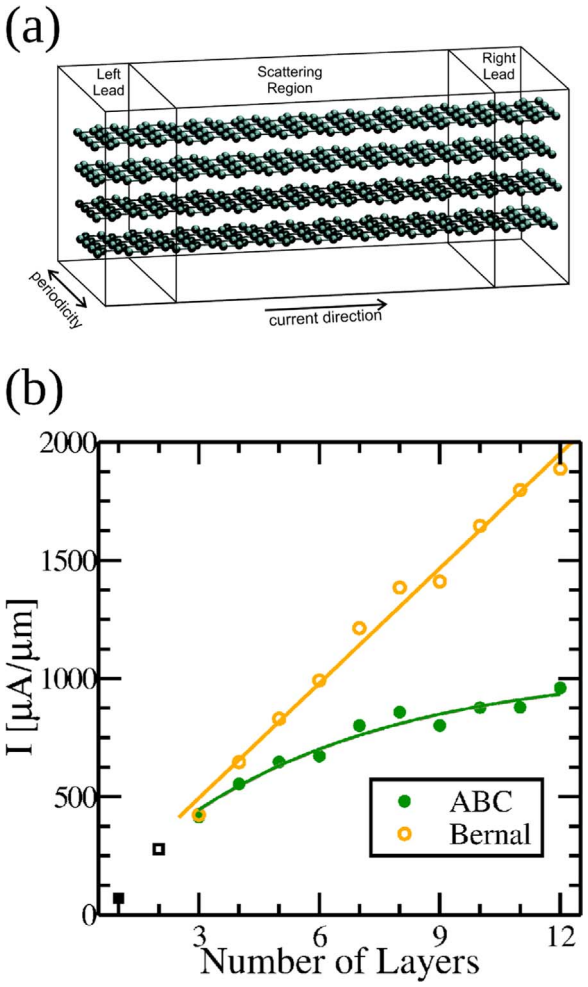

Fig. 2. (a) Schematic representation of the geometry used to perform the transport calculations. (b) Charge current per unit width as a function of the number of layers, for both AB and ABC stackings. The full (empty) square is associated with the calculated current for single (bilayer) graphene. The curve for the AB stacking is a linear fit whereas for the ABC stacking it is obtained from Eq. (2), as described in the text.

3. Results and discussions

In Fig. 2(b) we present the current as a function of the number of layers N, for up to 12 layers. It can be noticed that the current has a linear behavior with N for the Bernal stacking whereas it tends to saturate for the ABC stacking. Also, the current differences become even more pronounced as the number of layers increases, and a higher current for the Bernal stacking pattern is always observed. This indicates that the number of transport channels increases linearly with N for the Bernal configuration, whereas it tends to saturate in the ABC case.

This current behavior can be understood analysing the energy bands around the Fermi energy (E_F), which are highly sensitive to both the number of layers as well as the kind of stacking. In Fig. 3 (a) we show the energy bands and the Density Of States (DOS) for the Bernal stacking for N=8 layers. As can be seen, several energy bands cross the Fermi Level. Their number increases with N, explaining the source of the linear behavior of the current. However, small deviations from linearity occur due to splittings caused by anti-crossings of the energy bands close to the Fermi energy. Also, in Fig. 3(a), we present in the rightmost panel the charge density generated by states within an energy window of ± 0.1 eV around the Fermi Level. These states are delocalized over all layers, with a slight preference for the middle (bulk) region.

Thus, we can approximate the resistance ($R_{Bernal}(N)$) of an N layer

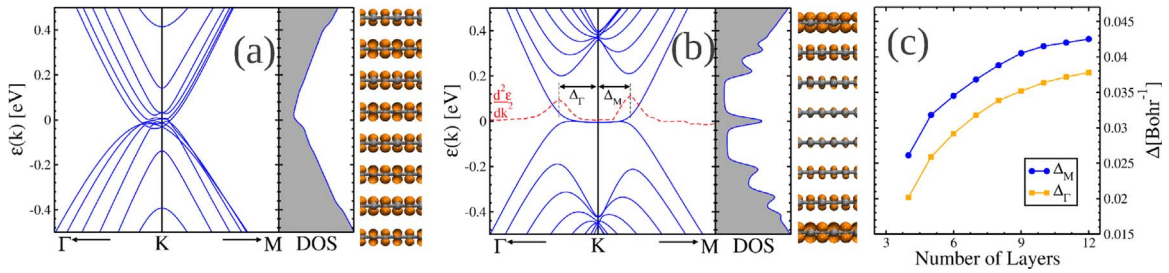

Fig. 3. Energy bands, Density of States (DOS), and the Local Density Of States (LDOS)—within an energy range of ± 0.1 eV around the Fermi Level—for the (a) AB and (b) ABC stacking patterns, for N=8 layers. In (c) we present Δ_M and Δ_Γ (see text for definitions) as a function of N for the ABC stacking pattern.

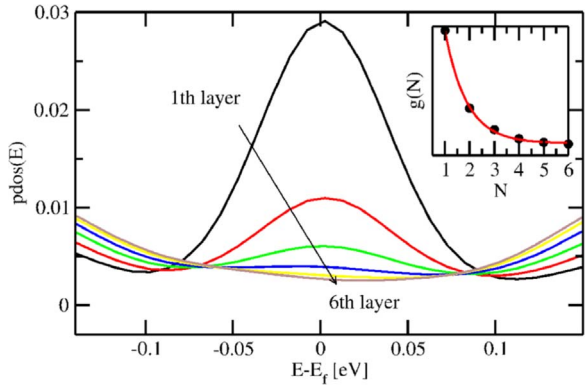

Fig. 4. Layer projected Density of States for a system with N=12 for the ABC stacking. Layer one is the outermost whereas layer 6 is the innermost one. Inset shows $g(N)$: the PDOS integrated within an energy window of ±0.05 eV around the Fermi level for each layer (N). Circles represent the calculated data, and the solid line is a fitting using the function $g(N) = Ae^{-BN} + C$.

Bernal stacking as resulting from the coupling of surface and bulk resistances in parallel:

$$1/R_{Bernal}(N) \simeq 2/R_S^B + N/R_0^B. \quad (1)$$

where $R_S{}^B$ and $R_0{}^B$ are the surface and bulk resistances per sheet, per lateral width. Those values were obtained through a linear fit of the I × N curve for the Bernal case, as presented in Fig. 2(b). The resulting values were $R_S^B = 1.23 \times^{-2}\ \Omega$m and $R_0^B = 3.08 \times 10^{-4}\ \Omega$m. Since $R_S{}^B$ is two orders of magnitude greater than $R_0{}^B$, it is possible to conclude that the bulk is the dominating transport channel for the AB systems. Furthermore, comparing $R_0{}^B$ with the single layer resistance ($7.2 \times 10^{-4}\ \Omega$m), it is found a considerable decreasing of the resistance per layer for the AB stacked systems, indicating that the interlayer combination of the π orbitals enhance the conductivity in comparison with a single layer.

The behavior of the current as well as the resistance is quite different for the ABC stacking. In Fig. 3(b) we present the band structure and DOS for the ABC stacking for N=8 layers. One feature is the presence of only one valence and one conduction band close to the Fermi level for any value of N. These bands have a flat region around the special K point close to the Fermi level, which is then connected to dispersive states. These flat regions are associated with surface states, as can be clearly seen in the local density of states (within an energy window of ±0.1 eV around the Fermi Level) presented in the rightmost panel of Fig. 3(b). Moreover, as N increases, these states becomes flatter, covering a larger region of k-points around K, leading to a more pronounced peak at the Fermi level. The dispersive parts of the bands are related to bulk-like states, as well as the higher and lower energy bands. As N increases, both the higher and lower bands get closer to the Fermi level, decreasing the bulk band-gap, indicating that for large enough N they will contribute with additional transport channels. For example, at room temperature, the bulk band-gap reaches the value of $k_BT = 0.025$ eV for N=50. Thus, the transport is dominated by surface states only up to a value of N=$N_S(T)$. For $N > N_S(T)$, the temperature will turn on some bulk states as active transport channels. However, for $N < N_S(T)$, we expected the current to be proportional to the k-points coverage. At the connection between the flat and the dispersive states, a pronounced increase in the curvature of the energy bands occur. Thus, this k-points coverage can be estimated using the peaks that will appear in the second derivative of the conduction band, as illustrated in Fig. 3(b). The positions of these peaks with respect to the K point along the Γ and M directions are defined here as Δ_Γ and Δ_M. They are shown in Fig 3(c) as a function of N. Both Δ_Γ and Δ_M will reach a limiting value corresponding to $N \to \infty$, indicating that the k-points coverage (and hence the current) will tend to saturate as N increases, as long as $N < N_S(T)$.

To obtain an approximate expression for the behavior of the resistance for the ABC stacking as a function of the number of layers N, we considered the spatial distribution of the states around the Fermi-level (E_f), as shown in the rightmost panel of Fig. 3(b). These states have a larger contribution at the outermost layers, with a progressively decreasing weight at the inner layers. All ABC stacked FLG present such a behavior. To obtain a more quantitative description, we analysed the layer projected DOS around the Fermi level for the N=12 system, as shown in Fig. 4. For the outermost layers there is a clear peak around E_F, within an energy window of ±0.08 eV. The increase of the PDOS beyond this window is due to the dispersive bands connected to the flat states. For the innermost layers the peak around E_F is almost inexistent. It is also clear that the height of the peak decreases as on moves towards the inner layers.

The inset in Fig. 4 shows the integrated PDOS around E_F within an energy window of ±0.025 eV. The solid line is a curve fitting using an exponential plus a constant expression. The fitting is excellent, indicating that there is an exponential decrease of the weight of the flat states towards the inner layers, plus a constant contribution, most likely connected to bulk like states. Based on these results, we construct a simplified model for the resistance of rhombohedral FLG considering resistances in parallel which (i) increase exponentially as one moves toward inner layers; and (ii) are symmetric with respect to the middle of the stacking. Such a dependence reads:

$$\frac{1}{R_{ABC}(N)} = \sum_{i=0}^{\frac{N}{2}-1} \frac{2}{R_0^{ABC} e^{\alpha i}} = \frac{2}{R_0^{ABC}} \frac{1 - e^{-\alpha \frac{N}{2}}}{1 - e^{-\alpha}}. \quad (2)$$

In this expression, R_0^{ABC} is the resistance of the surface layer, and α is the penetration factor. For large values of N, this expression predicts a saturation of $R_{ABC}(N)$ at $(1 - e^{-\alpha})R_0^{ABC}/2$. By using the *ab initio* data, we obtain $\alpha = 0.36$, and $R_0^{ABC} = 3.09 \times 10^{-4}\ \Omega$m. It is worth noting the impressive similarity between $R_0{}^B$ and R_0^{ABC} for the Bernal and the ABC stacking alignments. This resistance agreement provides a connection between the transport properties of these two alignments: The resistances for the Bernal FLGs are obtained by N equal resistances $R_0{}^B$ in parallel, one for each layer, whereas for the ABC FLGs the model of resistances in parallel is still valid, however the resistance of the i-th layer if $R_0^{ABC} e^{\alpha i}$.

Attempting an even better fitting for $R_{ABC}(N)$, we add a constant

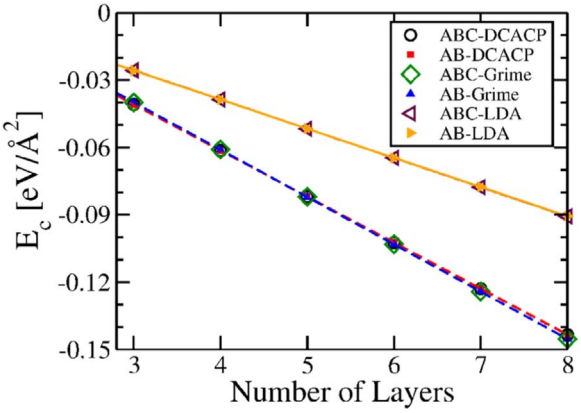

Fig. 5. Cohesive energy as a function of the number of layers for: LDA, GGA+DCACP and GGA+GRIMME functionals.

$1/R_B^{ABC}$ to Eq. (2), associated to an eventual N-independent bulk transport channel related to the constant C used to adjust $g(N)$. In this way we obtained $R_B^{ABC} = 5.4 \times 10^6\ \Omega$m, and no significant modifications in the values of α and R_0^{ABC}. This high resistance value indicates that no appreciable current will flow through an eventual N-independent bulk transport channel, or, in other words, the model of current concentrated at the outermost layers with an exponential penetration perfectly fits our calculated data.

In this way, from the electronic structure calculations we show how the electronic transport close to the charge neutrality point is related to surface states for the ABC FLGs. We predict that the current will tend to saturate up to $N \simeq N_S(T)$. For larger N, the current will start to increase again, due to the contribution from bulk states. On the other hand, for the Bernal stacking, the transport channels are delocalized over all layers, explaining the linear dependence of the current with N, as shown in Fig. 2 (b).

Despite both qualitative and quantitative differences on the transport properties, the same interlayer cohesive energies (E_c) [35] were observed for both kinds of stackings, as shown in Fig. 5. This is a remarkable result, since there is an electronic contribution to the total energy that depends on the band structure around the Fermi level, which are quite different for the two stacking orders (see Fig. 3 (a) and (b)). To attest the robustness of this result, we take attention to van der Waals interactions. The importance of these long range interactions in the description of total energy properties of layered graphene is well known. Thus, we carefully performed the cohesive energy calculations with two more methodologies beyond the LDA: (i) the Dispersion-Corrected Atom-Centred Potentials (DCACP) [36], as implemented by us in Ref. [37]. (ii) the Grimme [38] long range correction, as implemented in the VASP code [39]. Note that this latter methodology does not suffer from basis set superposition errors (BSSE). In order to coherently capture all advantages of each methodology, all geometries are separately relaxed within each methodology. The results presented in Fig. 5 show that both van der Waals corrected methodologies (DCACP and Grimme) present almost the same cohesive energy, with absolute differences less than 2 meV. These differences are mainly accounted for by the BSSE. Furthermore, the LDA calculations lead to a cohesive energy underbinding of ≃40%, proving that for an accurate description of the cohesive energy it is necessary to include long range, van der Waals interactions.

Despite differences in the absolute values, all levels of calculation revealed that the order of magnitude of the energy differences is within the limit of accuracy of the calculations, indicating that E_c is basically degenerated between the two stackings. Thus, we can conclude that there is no favourable stacking in such systems, and any observed preferences between these two stackings are probably connected to the growth conditions rather than to the energetics.

4. Conclusions

In conclusion, by performing *ab initio* electronic structure and transport calculations, we showed that both the electronic and transport properties of the few layer graphene are very sensitive to both the stacking sequence as well as the number of layers. For the ABC stacking the contribution to the transport is mainly due to surface states close to the Fermi level, connected to dispersive states with an exponential penetration toward the inner layers, whereas for the AB stacking the transport is evenly distributed over all the system. Since the electronic structure of the ABC FLG, close to the Fermi level, is largely dominated by surface states, this stacking configuration should be more sensitive to external perturbations, such as adsorption of atoms and molecules. As a result, more sensitive sensors could be constructed with this rhombohedral stacking of graphene. Moreover, the coupling of these FLG layers with other 2D materials, such as contacts, for example [7], should be also sensitive to the kind of stacking, since the interface properties should be quite different for the AB and ABC systems.

Acknowledgements

The authors thank the Brazilian funding agencies: CAPES, CNPq, FAPEG and FAPESP. We would like to acknowledge computing time provided by CENAPAD/Campinas-SP.

References

[1] J.M. Hamm, O. Hess, Science 340 (2013) 1298–1299.
[2] S.Z. Butler, S.M. Hollen, L. Cao, Y. Cui, J.A. Gupta, H.R. Gutirrez, T.F. Heinz, S.S. Hong, J. Huang, A.F. Ismach, E. Johnston-Halperin, M. Kuno, V.V. Plashnitsa, R.D. Robinson, R.S. Ruoff, S. Salahuddin, J. Shan, L. Shi, M.G. Spencer, M. Terrones, W. Windl, J.E. Goldberger, ACS Nano 7 (2013) 2898–2926.
[3] K.J. Koski, Y. Cui, ACS Nano 7 (2013) 3739–3743.
[4] A. Geim, I. Grigorieva, Nature 499 (2013) 419–425.
[5] M. Xu, T. Liang, M. Shi, H. Chen, Chem. Rev. 113 (2013) 3766–3798.
[6] G.S. Duesberg, Nature Matter 13 (2014) 1075–1076.
[7] J. Padilha, A. Fazzio, A.J. da Silva, Phys. Rev. Lett. 114 (2015) 066803.
[8] K.S. Novoselov, A.K. Geim, S. Morozov, D. Jiang, Y. Zhang, S. Dubonos, I. Grigorieva, A. Firsov, Science 306 (2004) 666–669.
[9] T.A. Nguyen, J.-U. Lee, D. Yoon, H. Cheong, Sci. Rep. 4 (2014) 4630.
[10] A. Reina, X. Jia, J. Ho, D. Nezich, H. Son, V. Bulovic, M.S. Dresselhaus, J. Kong, Nano Lett. 9 (2008) 30–35.
[11] J.B. Oostinga, H.B. Heersche, X. Liu, A.F. Morpurgo, L.M. Vandersypen, Nat. Matter 7 (2008) 151–157.
[12] C. Faugeras, A. Nerrire, M. Potemski, A. Mahmood, E. Dujardin, C. Berger, W.A. de Heer, Appl. Phys. Lett. (2008) 92.
[13] H.J. Park, J. Meyer, S. Roth, V. Skákalová, Carbon 48 (2010) 1088–1094.
[14] H. Min, A.H. MacDonald, Phys. Rev. B 77 (2008) 155416.
[15] R. Xiao, F. Tasnádi, K. Koepernik, J.W.F. Venderbos, M. Richter, M. Taut, Phys. Rev. B 84 (2011) 165404.
[16] S. Latil, L. Henrard, Phys. Rev. Lett. 97 (2006) 036803.
[17] Z. Li, C.H. Lui, E. Cappelluti, L. Benfatto, K.F. Mak, G.L. Carr, J. Shan, T.F. Heinz, Phys. Rev. Lett. 108 (2012) 156801.
[18] K.F. Mak, J. Shan, T.F. Heinz, Phys. Rev. Lett. 104 (2010) 176404.
[19] D. Pierucci, H. Sediri, M. Hajlaoui, J.-C. Girard, T. Brumme, M. Calandra, E. Velez-Fort, G. Patriarche, M.G. Silly, G. Ferro, V. Soulire, M. Marangolo, F. Sirotti, F. Mauri, A. Ouerghi, ACS Nano 9 (2015) 5432–5439.
[20] S.H. Jhang, M.F. Craciun, S. Schmidmeier, S. Tokumitsu, S. Russo, M. Yamamoto, Y. Skourski, J. Wosnitza, S. Tarucha, J. Eroms, C. Strunk, Phys. Rev. B 84 (2011) 161408.
[21] W. Bao, L. Jing, J. Velasco, Y. Lee, G. Liu, D. Tran, B. Standley, M. Aykol, S.B. Cronin, D. Smirnov, M. Koshino, E. McCann, M. Bockrath, C.N. Lau, Nat. Phys 7 (2011) 948–952.
[22] Y. Liu, W.S. Lew, S. Goolaup, H.F. Liew, S.K. Wong, T. Zhou, ACS nano 5 (2011) 5490–5498.
[23] J.P. Perdew, A. Zunger, Phys. Rev. B 23 (1981) 5048.
[24] J.M. Soler, E. Artacho, J.D. Gale, A. García, J. Junquera, P. Ordejón, D. Sánchez-Portal, J. Phys.: Condens. Matter 14 (2002) 2745.
[25] J.-C. Charlier, X. Gonze, J.-P. Michenaud, Carbon 32 (1994) 289–299.
[26] J.-C. Charlier, X. Gonze, J.-P. Michenaud, Phys. Rev. B 43 (1991) 4579–4589.
[27] Y. Baskin, L. Meyer, Phys. Rev. 100 (1955) 544.
[28] R. Landauer, Phil. Mag. 21 (1970) 863–867.
[29] M. Büttiker, Y. Imry, R. Landauer, S. Pinhas, Phys. Rev. B 31 (1985) 6207.
[30] Y. Meir, N.S. Wingreen, Phys. Rev. Lett. 68 (1992) 2512.
[31] M.P. Lima, A.J.R. da Silva, A. Fazzio, Phys. Rev. B 84 (2011) 245411.
[32] J.E. Padilha, M.P. Lima, A.J.R. da Silva, A. Fazzio, Phys. Rev. B 84 (2011) 113412.
[33] J.E. Padilha, R.B. Pontes, A.J. Da Silva, A. Fazzio, Int. J. Quant. Chem. 111 (2011)

1379–1386.
[34] F. Xia, D.B. Farmer, Y.-m. Lin, P. Avouris, Nano Lett. 10 (2010) 715–718.
[35] For a given FLG with N layers, and for a particular stacking, the cohesive energy per area is defined as $E_c = [E_{TOT}^{FLG}(N) - N \times E_{TOT}^{gr}]/S_{u.c.}$, where $E_{TOT}^{FLG}(N)$ (E_{TOT}^{gr}) is the total energy per unitary cell of a N layer FLG (single graphene layer), and $S_{u.c.} = a_{latt}^2 \cos(60°)$ is the area of the hexagonal unitary cell having a lattice parameter a_{latt}.
[36] I.-C. Lin, M.D. Coutinho-Neto, C. Felsenheimer, O.A. von Lilienfeld, I. Tavernelli, U. Rothlisberger, Phys. Rev. B 75 (2007) 205131.
[37] M.P. Lima, A. Fazzio, A.J. da Silva, Phys. Rev. B 79 (2009) 153401.
[38] S. Grimme, J. Comput. Chem. 27 (2006) 1787–1799.
[39] G. Kresse, J. Furthmüller, Phys. Rev. B 54 (1996) 11169–11186.